

The effect of beam section property on the behavior of modular prefabricated steel moment connection

Seyed Morteza Kazemi^{*1}, Mohammad Reza Sohrabi^{2a} and Hasan Haji Kazemi^{3b}

¹ Department of Civil Engineering, Kashmar Branch, Islamic Azad University, Kashmar, Iran

² Civil Engineering Department, University of Sistan and Baluchestan, Zahedan, Iran

³ Civil Engineering Department, Ferdowsi University, Mashhad, Iran

(Received April 22, 2019, Revised August 28, 2019, Accepted September 16, 2019)

Abstract. The specially prefabricated steel moment connections with pyramid head is one of the significant innovations in the steel structures forms to improve the installation time and simplify the construction procedure. The beams in this structure form are supported by two top and bottom angles and web double angles. Such a configuration despite its advantages increases the welding operation and filed installation time and costs. In this paper, the effect of using beams with channel and I section in three classes of seismically compact, seismically non-compact, and slender section according to width-to-thickness ratio on the behavior of the connection was investigated under monotonic and cyclic loading. Modeling was performed by ABAQUS and verified by the results of an experimental specimen. The findings indicated that using I and channel section instead of angle section reduces the amount of welding materials as well as easing the installation procedure. However, it has no significant effect on the ultimate strength and ductility of the connection. Furthermore, if the beam section is seismically compact, this form is considered as a special moment frame that has a rotation capacity up to 0.04 radians without any reduction in connection moment resistance.

Keywords: new connection; modular pre-fabricated structural form; cyclic loading; monotonic loading; I and channel beam section

1. Introduction

One of the important factors to improve the efficiency in construction industry is to use modern materials and new construction methods. The components of a prefabricated modular steel moment form are a tubular column and a beam with two top and bottom angles. At the end of each column, a horizontal connection plate and at the end of each beam, a short column was provided which is limited to the horizontal connection plates from each side. To simply assemble the beam to the column, a pyramidal end block was used on the connection plate of the lower-floor column that placed into the short column.

Several researchers such as Liu *et al.* (2015a, b, 2017a, b) and Kazemi *et al.* (2017, 2018) have studied this type of connection. Liu *et al.* (2015a, b, 2017a, b) investigated the effect of top, bottom, and web double angles' section property on the connection behavior. Additionally, the stress values and distribution in bolts were investigated and a method was proposed for assembling the beam with I-shaped cross-section. Kazemi *et al.* (2017) investigated the effect of connection plate thickness on the connection behavior. They also proposed a more convenient method for assembling the connection components.

In another study by Liu *et al.* (2018), they focused on a modular-prefabricated high-rise steel frame structure with diagonal braces and analyzed it using ETABS. In their work, the modular-prefabricated frame included pyramidal end block at the end of each column but it was not engaged in analytical calculations and numerical simulations. In 2018, Kazemi *et al.* (2018b) also proposed a new geometry of pyramidal end block for pre-fabricated moment connection and evaluated its behavior under monotonic and cyclic loadings. In another work in that year, they also studied the behavior of the mentioned connection with several cross-section shapes and plates with different thickness under cyclic loadings (Kazemi *et al.* 2018a). Liu *et al.* in another study in 2019 investigated the using of a bolted joint for connecting H-section steel beams to square hollow structural steel columns and connecting the upper and lower part of these columns in a multi-story prefabricated steel structure. They analyzed the models under cyclic loads using finite element method. The seismic performance of the connections, including the hysteretic behavior, skeleton curve, ductility, rotational capacity and stiffness degradation as well as the effect of the number of bolts and the thickness of cover plate on the mechanical and seismic properties were studied.

Regarding Fig. 1(a), the modular form proposed by Liu *et al.*, which is composed of top and bottom as well as web double angles, makes the fabrication procedure time-consuming and costly and Fig. 1(b) indicates the implementation process using the pyramidal end block. In this study, the effect of using beams in this structural form

*Corresponding author, Assistant Professor,

E-mail: kazemi@iaukashmar.ac.ir

^a Associated Professor, E-mail: sohrabi@hamoon.usb.ac.ir

^b Professor, E-mail: hkazemi@um.ac.ir

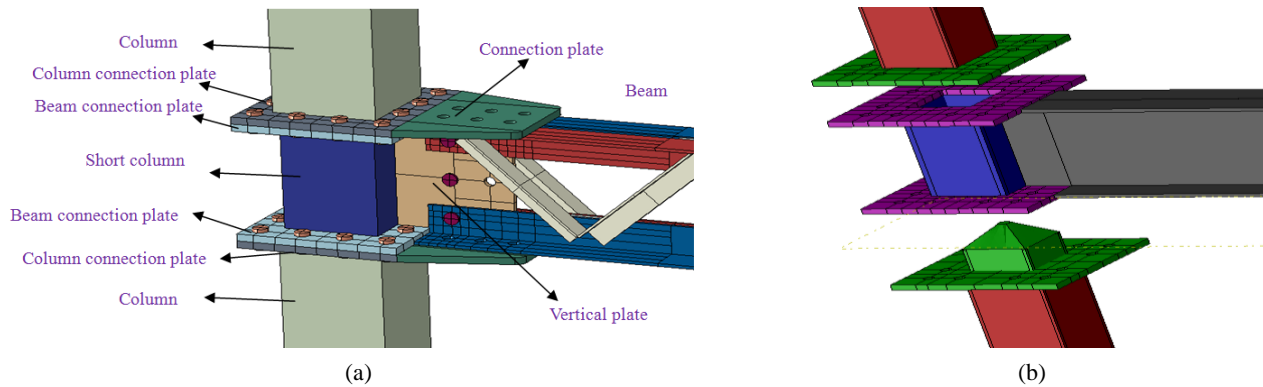


Fig. 1 (a) Components of the connection; (b) Implementation process of pyramidal end block

with I and channel section in three classes of seismically compact, seismically non-compact and slender section based on AISC was investigated under monotonic and cyclic loading. The results were compared with a form in which a beam with angle cross-section is used. In the current study, the monotonic loading was applied based on the load pattern in non-linear static pushover analysis for the entire specimens until it reaches $1.3M_p$ while cyclic loading was used according to SAC2000 protocol and it continues until one of the elements of the connection begin to fail (FEMA-350 2000).

Several experimental studies such as the works of Nair *et al.* (1974), Yang and Kim (2007), Pachoumis *et al.* (2009), Qin *et al.* (2014) and Bravo and Herrera (2014) have been performed while the laboratory facilities had been at hand. However, today, the finite element modeling leads the way in this field due to various reasons. While the numerical simulations by finite element methods are relatively cost-effective, the experimental studies have failed to precisely examine the local effects and develop the parametric framework. Thus, the finite element software packages have been widely used in this area by many researchers including Broderick and Thomson (2002), Zeinoddini *et al.* (2014), Shi *et al.* (2007), Ozel *et al.* (2017), Mashaly and El-Heweiety (2011) and Wang *et al.* (2016).

Maggi *et al.* in 2005 analyzed steel bolted end plate connections using finite element modeling using ANSYS. The main aspects discussed in that study were material nonlinearities, geometrical discontinuities and large displacements. For geometrical study, the end plate thickness and bolt diameter were selected as main variables. In a study done by Gray and McCarthy (2012), an analytical model was developed to reproduce the through-thickness stiffness of single-bolt, single-lap composite joints under secondary bending. The presented model can be used to decrease the time and cost of simulations in numerical models. Coelho in 2013 studied a partial strength steel joint behavior confined to the end plate connection using finite element analyses. The investigation included the connection behavior with variations in beam depth and thickness of the end plate.

Brunesi *et al.* in three different studies investigated the behavior of partially-restrained bolted beam-to-column connections under seismic loads in modern steel moment

resisting frames. The first one in 2014 focused on geometric variations in the connection system by using NX Nastran solver and FEMAP as the pre- and post-processing software. In the second research in that year, they investigated the beam-bolts-plates-column structural chain in bolted top-and-seat angle connection using finite element method. Global responses such as failure mechanisms, ductility capacity and dissipation energy capabilities were studied. In their third work in 2015, a simplified FE model of T-stub connection was developed to assess its seismic performance in four- and eight-story frames and the results were compared to those for other top-and-seat angle joints investigated in the past research program.

In this study, the experimental model of Liu *et al.* (2015a) research project was reproduced and verified using ABAQUS and then the specimen was developed for new investigation.

2. FE Model verification and development

The numerical model of the connection studied in this research is adopted from experimental specimen of Liu *et al.* (2015a). The connection is composed of tubular columns, truss beam as well as the connection and vertical plates. In this type of connection, a truss beam is bolted to the connection and vertical plates which are then welded to column connection plates and a short column respectively. The vertical plates are then connected to the beam web using another bolted vertical plates. The upper and lower story columns are assembled by means of plates and the short column in a way that the columns are welded to the column connection plates which are then bolted to the beam connection plates in the field. The short column plays the role of medium component to which vertical plates and beam connection plates are welded. For all of the components, Q235B steel, S10.9 bolts, and standard holes were used. Pre-tension force was applied to all bolts according to the types and sizes of the bolts (Salmon *et al.* 2008). The friction coefficient of the bolts with the connection plates was set to 0.303 that is the average value of three friction test that were 0.29, 0.30 and 0.32 (JGJ82 2011). The size and dimension of the connection components have been chosen similar to the specimen of Liu *et al.* (2015a). Figs. 2 and 3 show the force-displacement

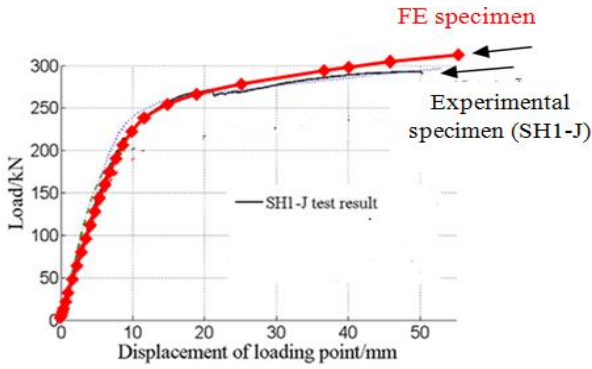


Fig. 2 Force-displacement curves for experimental and FE specimens

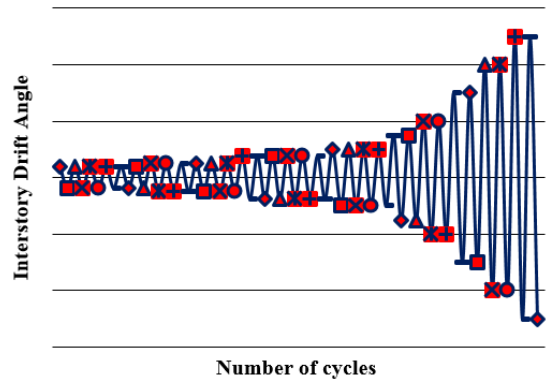
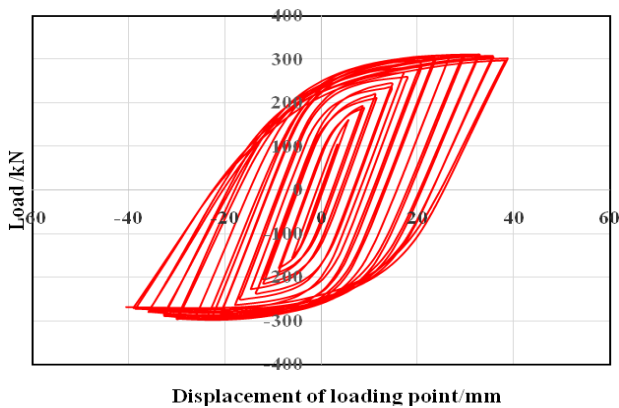
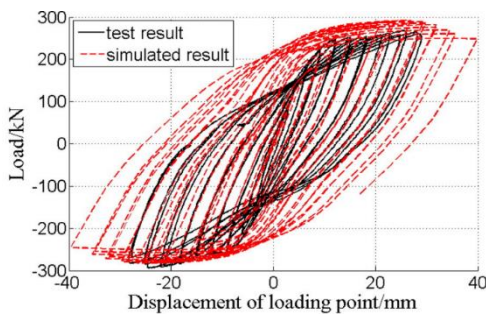


Fig. 4 FEMA/SAC2000 loading protocol in accordance with FEMA350 (FEMA-350 2000)



(a) FE specimen



(b) Experimental specimen

Fig. 3 Force-displacement curves for experimental and FE specimens under cyclic loading: (a) FE results of the current study; (b) FE and Experimental results of Liu *et al.* (2015a) study

curves of the specimen and its FE model. Yielding force (P_y) of SH1-J specimen and FE model are 162.99 kN and 164.6 kN respectively, which differ by one percent. Fig. 3(a) represents the force-displacement curve of the current study while Fig. 3(b) belongs to Liu *et al.* (2015a) research projects. The FE results show an acceptable agreement and they are close to the experimental data. It is evident that the difference between FE results and experimental data comes from several factors including bolts slippage and plates interactions that cannot be simulated exactly to what happens during the experiment and is common in most FE

Table 1 Cyclic loading according to SAC protocol

Step	Peak deformation θ (rad.)	Number of cycles	Beam end displacement (mm)
1	0.00375	6	± 9.1875
2	0.005	6	± 12.25
3	0.075	4	± 18.375
4	0.01	2	± 24.5
5	0.015	2	± 36.75
6	0.02	2	± 49
7	0.03	2	± 73.5

*continue with increments of 0.01 for θ and perform two cycles in each step

studies.

After verification, the model was developed for further investigation. To this aim, all of the specimens applied under monotonic loading and cyclic loading. In monotonic loading, a point load was applied at the end of the beam and the amount of the loading started from zero and increased to a certain amount with increments of 1 kN.

In cyclic loading, loads are applied through controlling displacements at the end of beam according to SAC2000 (FEMA-350 2000). The values are shown in Table 1 and Fig. 4.

3. Material properties and dimension of connection components

For all specimens, St37 steel has been used with modulus of elasticity 200 Gpa. The Material properties used in FE modeling are shown in Figs. 5 and 6. The size and dimension of connection components are shown in Fig. 7 which is identical to those used in Kazemi *et al.* (2018b). It should be noted that the dimension of the beam and column was selected due to their favorable performance in FE simulations and their suitability for the objectives of this study.

In all specimens, the beam was directly connected to the plates that caused the failure to begin from the connection zone. For this reason, the use of top and bottom plates was

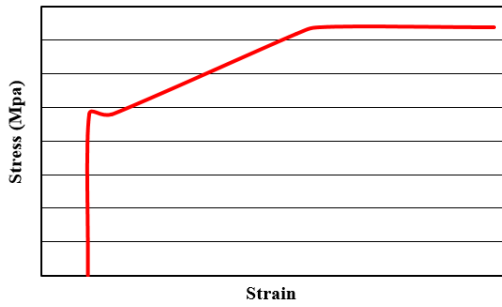


Fig. 5 Material properties of sections used in FE modeling (Gerami *et al.* 2010)

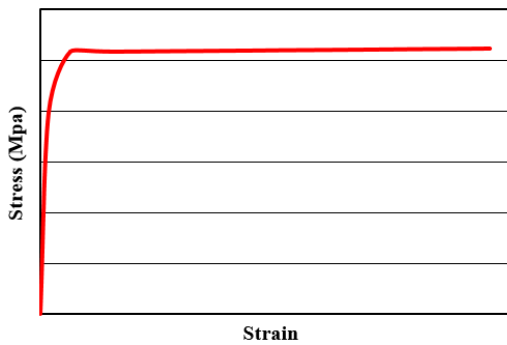


Fig. 6 Material properties of bolts used in FE modeling (Gerami *et al.* 2010)

proposed to strengthen the beam to column connection. Fig. 8 shows the top and bottom plates as well as beam to column connection (the vertical plates dimension are identical to what was presented in Fig. 7). As it can be seen, the top and bottom plates were connected to the beam by six 16 mm diameter bolts and welded to the connection plates.

4. Modeling

In this section, the effect of the beam section as well as its type of connection to the plates on the overall behavior of the connection was investigated through using I and channel section in three classes of seismically compact, seismically non-compact, and slender element section. The type of element was determined according to AISC (Eqs. (1) to (3) for seismically compact, seismically non-compact, and slender element section respectively). The name and properties of the specimens are presented in Table 2. In this table, C stands for connection and the following number is the number of specimen. Here, L, I and U represent the shape of the beam cross-section that are angle, I-section (IPE) and channel (UNP) respectively. The letter C, NC and S also stand for seismically compact, seismically non-compact, and slender section. In C8ICPL, the beam is connected to the connection plates using bolted top and bottom plates.

$$\frac{b}{t} < 0.37 \sqrt{\frac{E}{F_y}} \tag{1}$$

$$0.3 \sqrt{\frac{E}{F_y}} < \frac{b}{t} < 0.37 \sqrt{\frac{E}{F_y}} \tag{2}$$

$$\frac{b}{t} > 0.37 \sqrt{\frac{E}{F_y}} \tag{3}$$

Fig. 9 indicates the parameters relating to the geometry of the components. The meshing details are also shown in Fig. 10. As it can be seen, the finer mesh was applied to the regions that require more precision.

The load-displacement curves under monotonic and cyclic loading for different specimens in various conditions are also indicated in Figs. 11 to 17. Fig. 18 shows von Mises

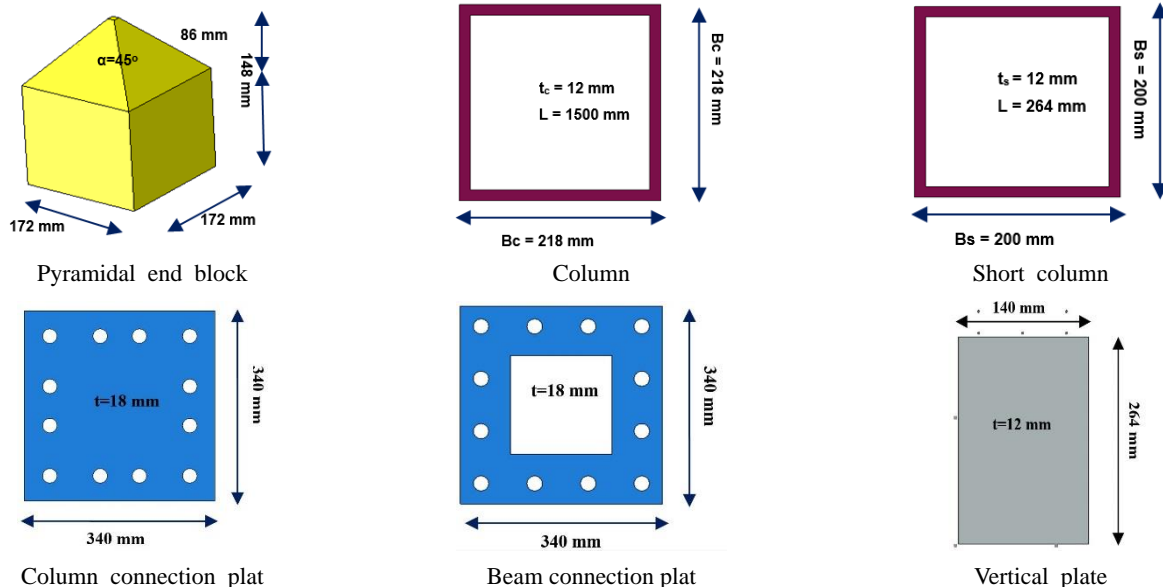


Fig. 7 Size and dimension of connection components

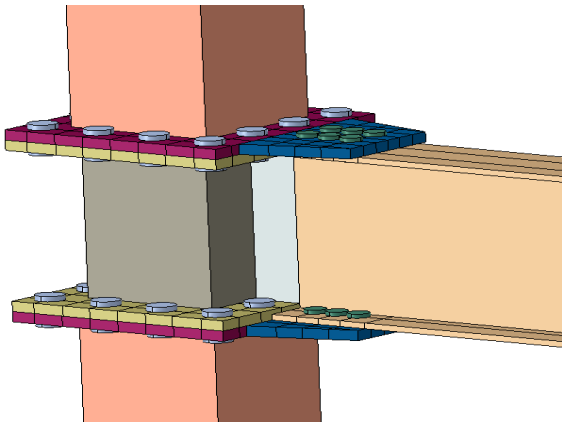


Fig. 8 Details connection set-up and beam to the connection plates with bolted top and bottom plates

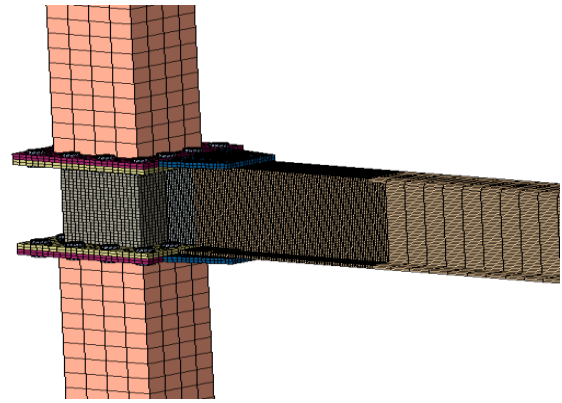


Fig. 10 Meshing details of the connection components

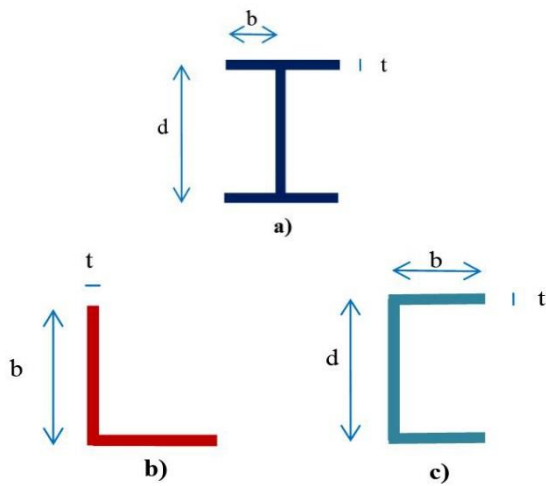


Fig. 9 Parameters relating to the geometry of the components: (a) I section; (b) Angle section; and (c) Channel section

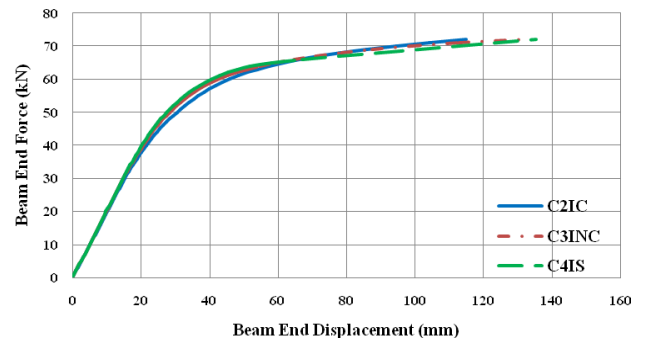


Fig. 11 Force-displacement curves under monotonic loading for specimens with I- shape cross-section beams

stress contour of the specimens. Table 3 presents the displacement values resulted from service load (D_s) and at the time when the applying load at the end of the beam reaches up to 72 kN (D_{72}) in which the applied moment to the connection is equal to 1.3 beam plastic moment (M_p).

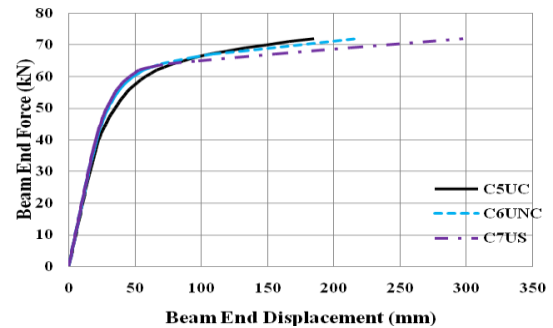


Fig. 12 Force-displacement curves under monotonic loading for specimens with channel-shape cross-section beams

Table 2 Summary of specimen details

Specimens	Beam section	b (mm)	t (mm)	d (mm)	tw (mm)	Z (cm ³)	Beam to plates connection type
C1LNC	angle	80	7.4	-	-	573	weld
C2IC	IPE	65	10	300	10	573	weld
C3INC	IPE	81.75	8	300	9.5	573	weld
C4IS	IPE	90	7.3	300	9.25	573	weld
C5UC	UNP	65	10	300	5	573	weld
C6UNC	UNP	81.75	8	300	4.75	573	weld
C7US	UNP	90	7.3	300	4.625	573	weld
C8ICPL	IPE	65	10	300	10	573	Plate + bolt

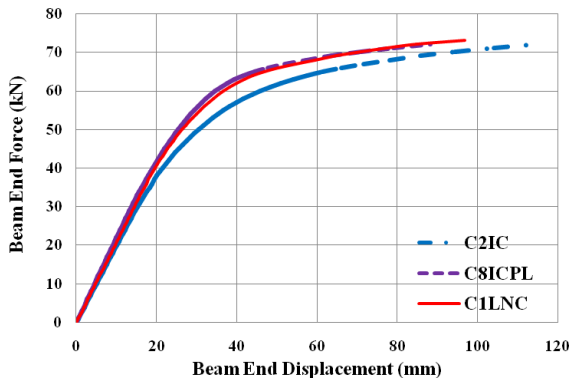


Fig. 13 Force-displacement curves under monotonic loading for C1LNC, C2IC and C8ICPL

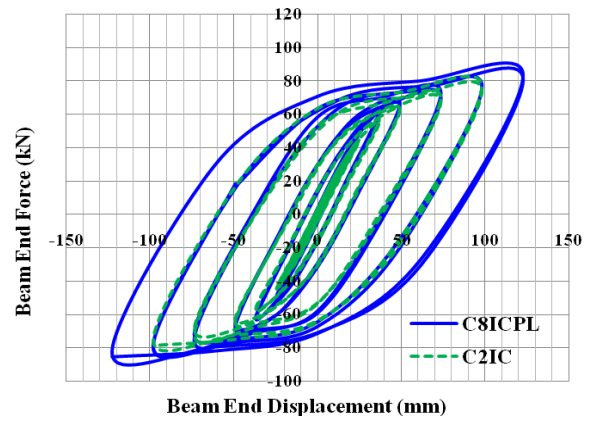


Fig. 17 Force-displacement curves under cyclic loading for specimens with and without top and bottom plates

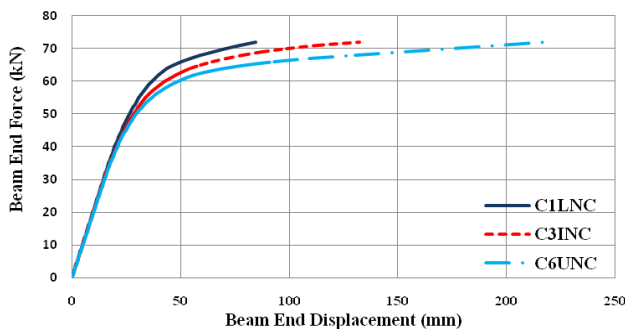


Fig. 14 Force-displacement curves under monotonic loading for seismically non-compact specimens

Table 3 D_s and D_{72} values for different specimens

Specimens	D_s (mm)	D_{72} (mm)
C1LNC	14.4713	84.7685
C2IC	15.298	115.008
C3INC	14.843	132.204
C4IS	14.7086	135.44
C5UC	15.8855	185.386
C6UNC	15.0186	217.38
C7US	14.8871	297.9
C8ICPL	13.73	88.2997

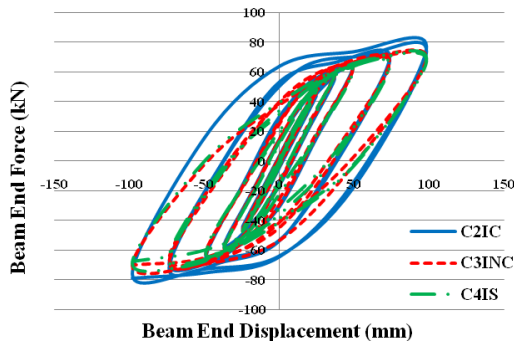


Fig. 15 Force-displacement curves under cyclic loading for specimens with I- shape cross-section beams

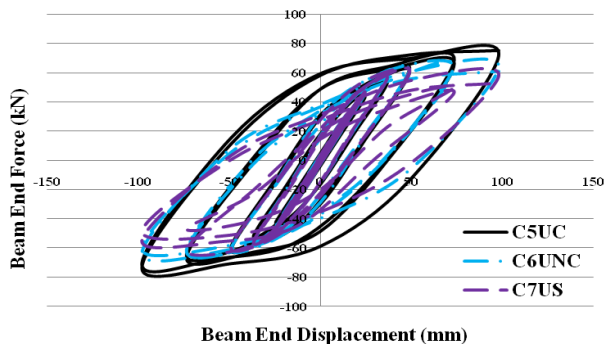


Fig. 16 Force-displacement curves under cyclic loading for specimens with channel-shape cross-section beams

For C2IC, as the value of applied force at the end of the beam reaches 31 kN and the corresponding displacement is 15.85 mm, a region of the connection plates yields and as the applied force becomes 72 kN and the corresponding displacement reaches 115 mm, a full plastic hinge forms in the beam. As it can be seen in Fig. 12, for C5UC, the amount of force that causes the first part of the connection to be yielded is equal to 41 kN and the corresponding displacement is 23.24 mm. These values for C6UNC and C7US are 37 kN and 19.022 mm as well as 36 kN and 18.11 mm respectively.

As it can be seen in Figs. 11 to 18, the entire specimens can bear a displacement up to 98 mm (0.04 radians) except C8ICPL which went under 122.5 mm (0.05 radians) without having any significant reduction in its flexural strength. This shows a high ductility of such a structural form. However, in specimens that are seismically non-compact and slender, the beam experiences lateral deflection and lost its flexural capacity. The connection of beam to the connection plates through top and bottom plates increases not only the ductility of the connection but also the stiffness of structure and makes the plastic hinge develop away from top and bottom plates.

Regarding the fact that the sections of steel frames are mostly made out of thin-wall sheets, they undergo local instability under applied compression forces. The compression stress in beams is caused by the applied

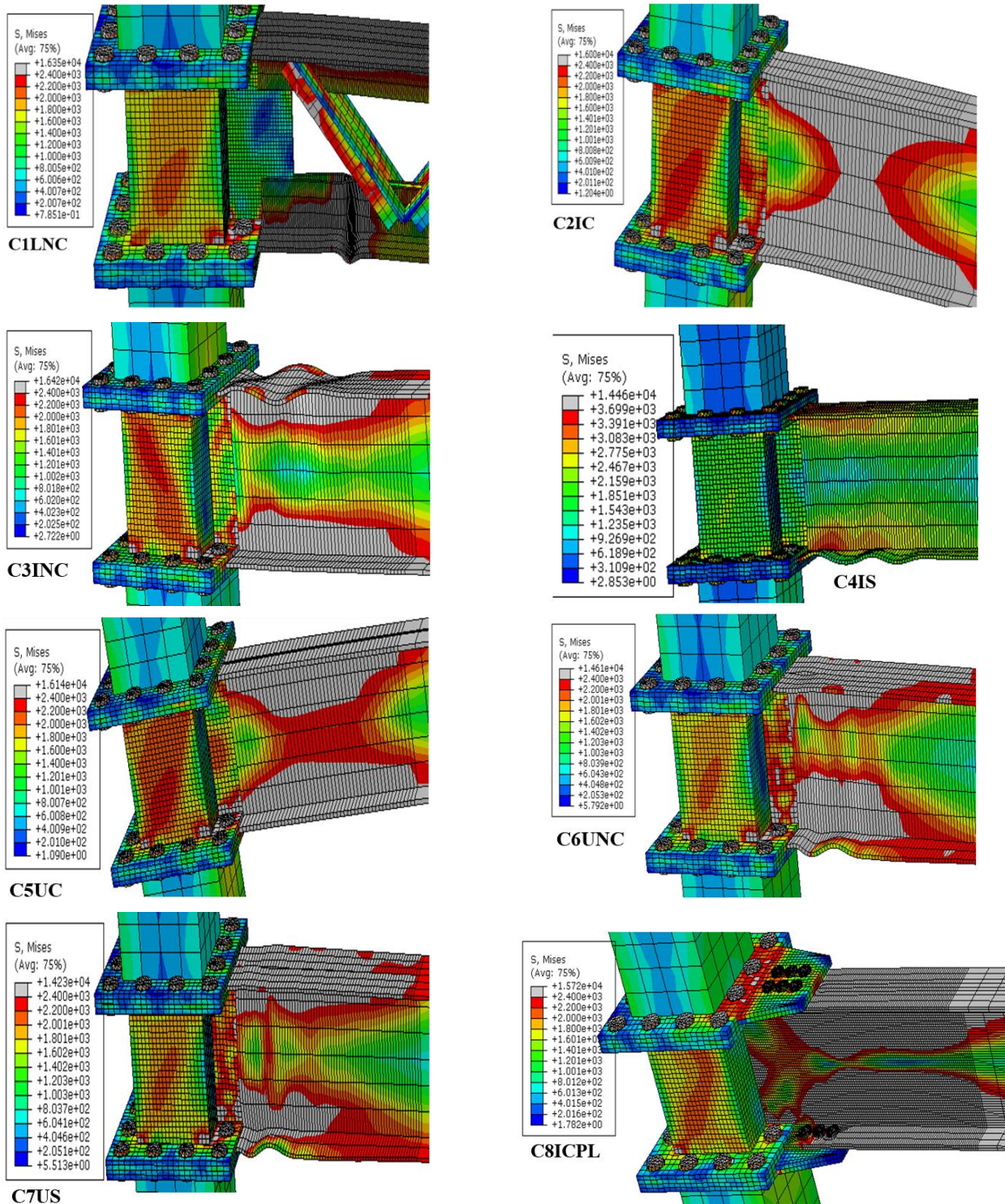


Fig. 18 Contour plot for Von Mises stress distribution in different specimens

moments. Since the resistance of the section against the applied stress depends on its capability in preventing the local instability of sheets, it is always necessary for the critical stress of the sheets, which are formed the section, to be higher than the yielding force with a sufficient safety factor to ensure the prevention of local instability. The sheets formed the compact sections under compression stress experience strains up to several times higher than yielding strain. These sections can enter into inelastic range

and the sheet capacity can be determined based on the theory of plasticity.

The sheets form the non-compact and slender element sections are incapable of entering into inelastic region and thus their capacity is determined by elasticity theory. As seen in Figs. 11 to 18, in case that the beam section is not compact, the connection strength decreases, the amount of displacement at the end of the beam under a constant force increases and the local buckling happens in the flange of the

beams. These effects are accentuated in case that the beam section is a slender element. For the beam with non-compact and slender I-section, the connection strength compared with the compact section is 10.7 and 14.8 percent respectively. This value for the channel section is 18.6 and 25.6 percent respectively.

5. Skeleton curve

One of the important curves that represent the behavior of connections is skeleton curve that describes the

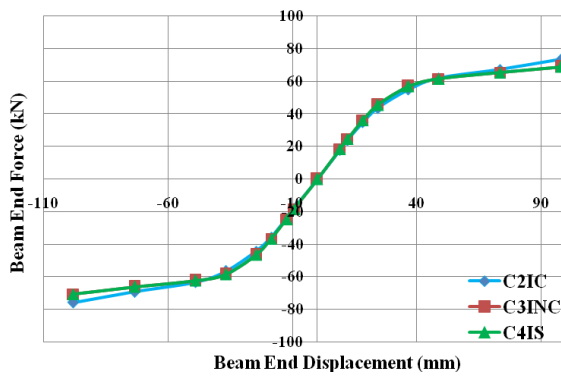


Fig. 19 Skeleton curves for specimens with I- shape cross-section beams

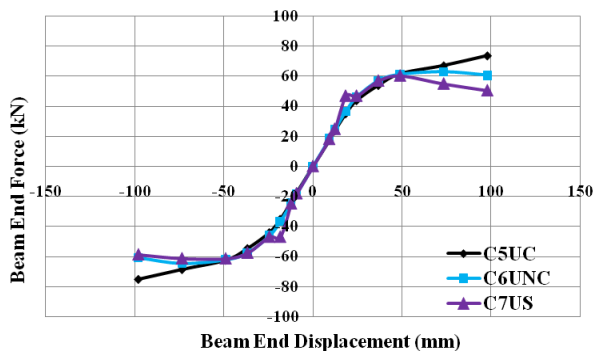


Fig. 20 Skeleton curves for with channel- shape cross-section beams

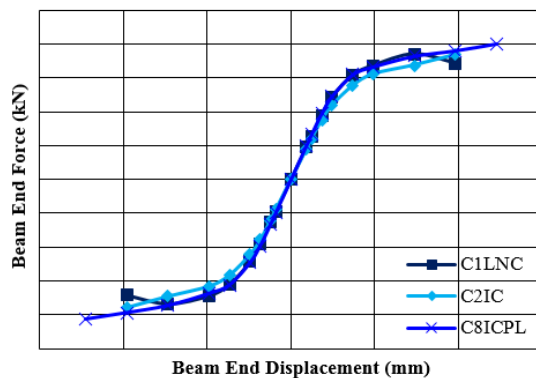


Fig. 21 Skeleton curves for C1LNC, C2IC and C8ICPL

relationship, upon first loading, between the applied load and the resulting displacement at the point of applying load (Elnashai *et al.* 1998). Figs. 19 to 21 show the skeleton curves of different specimens. In order to study a ductile moment resisting frame based on AISC provisions and its flexural strength, the moment-rotation curves of the entire specimens and the corresponding line to 80 percent of M_p of the beam were drawn in Figs. 22 to 24. In case that the strength of the connection at 4 percent of rotation is more than 80 percent of M_p , it satisfies the criteria of AISC Seismic Provisions for special moment frame systems.

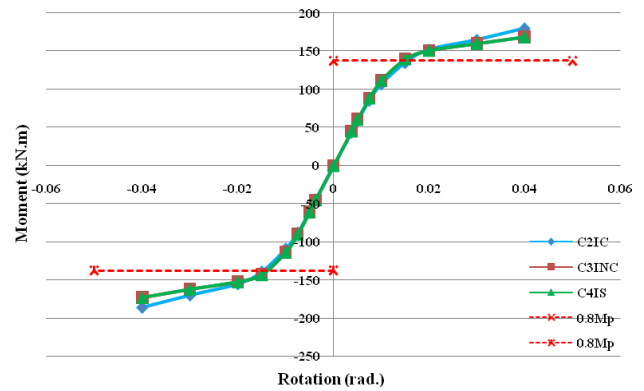


Fig. 22 Moment – Rotation skeleton curves for specimens with I- shape cross-section beams

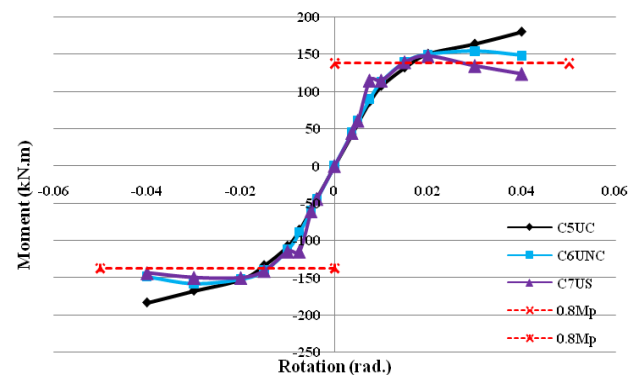


Fig. 23 Moment – Rotation skeleton curves for specimens with channel- shape cross-section beams

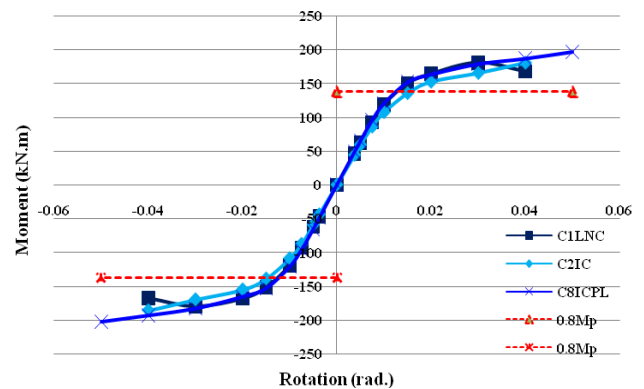
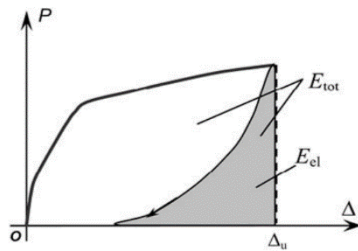


Fig. 24 Moment – Rotation skeleton curves for C1LNC, C2IC and C8ICPL

Fig. 25 Value of E_{tot} and E_{el} Table 4 E_{tot} , E_{el} and μ values for different specimens

Specimens	E_{tot} (kN.mm)	E_{el} (kN.mm)	μ
C1LNC	5552.7	1242	2.73
C2IC	5203.4	1396.6	2.36
C3INC	5143.5	1550.4	2.16
C4IS	5068.5	1528.8	2.16
C5UC	5160	1433.2	2.3
C6UNC	4972.5	1351.5	2.34
C7US	4705	1235.1	2.4
C8ICPL	7554.5	1625.2	2.82

As it can be seen in Figs. 19 to 24, the entire specimens except C7US experienced a rotation of 0.04 radians without any decrease in the flexural strength of the connections. In C7US, the case was different, the specimen lost its flexural strength at the rotation of 0.03 radians, and the resisting moment of the connection was lower than 80 percent of plastic moment.

6. Ductility index

As it is shown in Fig. 25, the ductility of specimens was measured using Eq. (4) according to Naaman and Jeong ductility index that is based on energy dissipation (Naaman and Jeong 1995). The results, which are presented in Table 4, indicate that employing seismically compact slender section reduces the ductility of the connection except in C7US in which the load-displacement curve dropped at the rotation of 0.03 radians. Furthermore, it was observed that using top and bottom plates increases the ductility of the connection.

$$\mu = 0.5 \left(\frac{E_{tot}}{E_{el}} + 1 \right) \quad (4)$$

7. Conclusions

In this paper, the effect of beam section property was investigated on the behavior of modular prefabricated moment connection under monotonic and cyclic loading. To this aim, an experimental specimen was modeled in ABAQUS and then verified through comparing the numerical outcomes with the experimental results. The main findings are as follows:

- Using the slender and seismically non-compact I-section instead of seismically compact I-section increases the beam end displacement up to 2.94 and 3.8 percent respectively under service loads and up to 14.95 and 17.8 percent under the loads developing 1.3 Mp at the beam. These values are 5.5 and 6.3 as well as 17.3 and 60.7 percent for channel section (UNP) respectively.
- Employing angle section (L-shaped cross-section) as a beam in this type of structures has some limitations including heavy work of welding and time-consuming installation. On the contrary, using channel and I section reduces the welding operation and filed installation time and costs. However, these sections have no significant effect on the ultimate strength and ductility of the connection.
- In case that the beam section does not meet the seismic requirements, it goes under local buckling during cycling loading and reduces the ultimate strength and capacity of the connection.
- Providing the seismic requirements for the beam section can expand the rotation capacity of the connection to 0.04 radians without any decrease in its ultimate strength and promotes the frame to special moment frame.

Welding the connection plates directly to the beam develops the maximum stress value at the connection that causes the failure of all specimens at this point. Thus, employing top and bottom plates to connect the beam to the connection plates not only makes the plastic hinge develop further than the side of the column and beyond the connection plates but also increases the ductility, rotation and strength capacity of the connection up to 20, 25 and 9.2 percent respectively.

References

- Bravo, M.A. and Herrera, R.A. (2014), "Performance under cyclic load of built-up T-stubs for Double T moment connections", *J. Constr. Steel Res.*, **103**, 117-130. <https://doi.org/10.1016/j.jcsr.2014.08.005>
- Broderick, B.M. and Thomson, A.W. (2002) "The response of flush end-plate joints under earthquake loading", *J. Constr. Steel Res.*, **58**(9), 1161-1175. [https://doi.org/10.1016/S0143-974X\(01\)00073-6](https://doi.org/10.1016/S0143-974X(01)00073-6)
- Brunesi, E., Nascimbene, R. and Rassati, G.A. (2014a), "Response of partially-restrained bolted beam-to-column connections under cyclic loads", *J. Constr. Steel Res.*, **97**, 24-38. <https://doi.org/10.1016/j.jcsr.2014.01.014>
- Brunesi, E., Nascimbene, R. and Rassati, G.A. (2014b), "Seismic Performance of Steel MRFs with Partially-Restrained, Bolted, Beam-to-Column Connections through FE Simulations", *Structures Congress 2014*, pp. 2640-2651.
- Brunesi, E., Nascimbene, R. and Rassati, G.A. (2015), "Seismic response of MRFs with partially-restrained bolted beam-to-column connections through FE analyses", *J. Constr. Steel Res.*, **107**, 37-49. <https://doi.org/10.1016/j.jcsr.2014.12.022>
- Coelho, A.M.G. (2013), "Rotation capacity of partial strength steel joints with three-dimensional finite element approach", *Comput. Struct.*, **116**, 88-97. <https://doi.org/10.1016/j.compstruc.2012.10.024>

- Elnashai, A.S., Elghazouli, A.Y. and Denesh-Ashtiani, FA. (1998), "Response of semi rigid steel frames to cyclic and earthquake loads", *J. Struct. Eng.*, **124**(8), 857-867.
[https://doi.org/10.1061/\(ASCE\)0733-9445\(1998\)124:8\(857\)](https://doi.org/10.1061/(ASCE)0733-9445(1998)124:8(857))
- FEMA (2000), Recommended seismic design criteria for new steel moment frame buildings, Report no. FEMA-350; Federal Emergency Management Agency: California Universities for Research in Earthquake Engineering.
- Gerami, M., Saberli, H., Saberli, V. and Saedi Daryan, A. (2010), "Cyclic behavior of bolted connections with different arrangement of bolts", *J. Constr. Steel Res.*, **67**, 690-705.
<https://doi.org/10.1016/j.jcsr.2010.11.011>
- Gray, P.J. and McCarthy, C.T. (2012), "An analytical model for the prediction of through-thickness stiffness in tension-loaded composite bolted joints", *Compos. Struct.*, **94**(8), 2450-2459.
<https://doi.org/10.1016/j.compstruct.2012.02.011>
- JGJ82-2011, (2011), Technical Specification for High Strength Bolt Connections of Steel Structure, China Building Industry Press; Beijing, China. [In Chinese]
- Kazemi Torbaghan, M., Sohrabi, M. and Haji Kazemi, H. (2017), "Study of BSB Connections Behavior under Cyclic Loads", *J. Struct. Steel*, **13**(20), 31-43.
- Kazemi, M.K., Sohrabi, M.R. AND Kazemi, H.H. (2018a), "Investigating the behavior of specially pre-fabricated steel moment connection under cyclic loading", *Adv. Steel Constr.*, **14**(3), 412-423.
<https://doi.org/10.18057/IJASC.2018.14.3.6>
- Kazemi, S.M., Sohrabi, M.R. and Kazemi, H.H. (2018b), "Evaluation the behavior of pre-fabricated moment connection with a new geometry of pyramidal end block under monotonic and cyclic loadings", *Steel Compos. Struct., Int. J.*, **29**(3), 391-404. <https://doi.org/10.12989/scs.2018.29.3.391>
- Liu, X., Pu, S., Zhang, A., Xu, A., Ni, Z., Sun, Y. and Ma, L. (2015a), "Static and seismic experiment for bolted-welded joint in modularized prefabricated steel structure", *J. Constr. Steel Res.*, **115**, 417-433. <https://doi.org/10.1016/j.jcsr.2015.08.036>
- Liu, X., Xu, A., Zhang, A., Ni, Z., Wang, H. and Wu, L. (2015b), "Static and seismic experiment for welded joints in modularized prefabricated steel structure", *J. Constr. Steel Res.*, **112**, 183-195.
<https://doi.org/10.1016/j.jcsr.2015.05.003>
- Liu, X., Pu, S., Zhang, A. and Zhan, X. (2017a), "Performance analysis and design of bolted connections in modularized prefabricated steel structures", *J. Constr. Steel Res.*, **133**, 360-373. <https://doi.org/10.1016/j.jcsr.2017.02.025>
- Liu, X.C., Yang, Z.W., Wang, H.X., Zhang, A.L., Pu, S.H., Chai, S.T. and Wu, L. (2017b), "Seismic performance of H-section beam to HSS column connection in prefabricated structures", *J. Constr. Steel Res.*, **138**, 1-16.
<https://doi.org/10.1016/j.jcsr.2017.06.029>
- Liu, X., Zhou, X., Zhang, A., Tian, C., Zhang, X. and Tan, Y. (2018), "Design and compilation of specifications for a modular-prefabricated high-rise steel frame structure with diagonal braces. Part I: Integral structural design", *Struct. Des. Tall Special Build.*, **27**(2), e1415.
<https://doi.org/10.1002/tal.1415>
- Liu, X.C., Cui, F.Y., Zhan, X.X., Yu, C. and Jiang, Z.Q. (2019), "Seismic performance of bolted connection of H-beam to HSS-column with web end-plate", *J. Constr. Steel Res.*, **156**, 167-181.
<https://doi.org/10.1016/j.jcsr.2019.01.024>
- Maggi, Y.I., Gonçalves, R.M., Leon, R.T. and Ribeiro, L.F.L. (2005), "Parametric analysis of steel bolted end plate connections using finite element modeling", *J. Constr. Steel Res.*, **61**(5), 689-708. <https://doi.org/10.1016/j.jcsr.2004.12.001>
- Mashaly, E. and El-Hewewity, M. (2011), "Finite element analysis of beam to-column joints in steel frames under cyclic loading", *Alexandria Eng. J.*, **50**(1), 91-104.
<https://doi.org/10.1016/j.aej.2011.01.012>
- Naaman, A.E. and Jeong, S.M. (1995), "Structural Ductility of Concrete Beams Prestressed with FRP Tendons, Nonmetallic (FRP) Reinforcement for Concrete Structures", *Proceeding of the Second International RILEM Symposium (FRPRCS-2)*, London, UK, pp. 379-389.
- Nair, R.S., Birkemoe, P.C. and Munse, W.H. (1974), "Hight strength bolts subject to tension and prying", *J. Struct. Div.*, **100**(2), 351-37.
- Ozel, H.F., Saritas, A. and Tasbahji, T. (2017), "Consistent matrices for steel framed structures with semi-rigid connections accounting for shear deformation and rotary inertia effects", *Eng. Struct.*, **137**, 194-203.
<https://doi.org/10.1016/j.engstruct.2017.01.070>
- Pachoumis, D.T., Galoussis, E.G., Kalfas, C.N. and Christitas, A.D. (2009), "Reduced beam section moment connections subjected to cyclic loading: Experimental analysis and FEM simulation", **31**(1), 216-223.
<https://doi.org/10.1016/j.engstruct.2008.08.007>
- Qin, Y., Chen, Z. and Wang, X. (2014), "Experimental investigation of new internal-diaphragm connections to CFT columns under cyclic loading", *J. Constr. Steel Res.*, **98**, 35-44.
<https://doi.org/10.1016/j.jcsr.2014.02.014>
- Salmon, C.G., Johnson, J.E. and Malhas, F.A. (2008), *Steel Structure Design and Behavior*, (5rd ed.), Prentice Hall, Publisher, New York, NY, USA.
- Shi, G., Shi, Y. and Wang, Y. (2007), "Behaviour of end-plate moment connections under earthquake loading", *Eng. Struct.*, **29**(5), 703-716. <https://doi.org/10.1016/j.engstruct.2006.06.016>
- Wang, H., Yang, B., Zhou, X.H. and Kang, S.B. (2016), "Numerical analyses on steel beams with fin-plate connections subjected to impact loads", *J. Constr. Steel Res.*, **124**, 101-112.
<https://doi.org/10.1016/j.jcsr.2016.05.016>
- Yang, C.M. and Kim, Y.M. (2007) "Cyclic behavior of bolted and welded Beam-to-Column joints", *J. Mech. Sci.*, **49**, 635-649.
<https://doi.org/10.1016/j.ijmecs.2006.09.022>
- Zeinoddini, V., Ghassemieh, M. and Kiani, M. (2014), "Finite element analysis of flush end plate moment connections under cyclic loading", *Int. J. Civil Architect. Sci. Eng.*, **8**(1), 96-104.

CC